

**Chaos in geodesic motion around a black ring**Takahisa Igata,<sup>\*</sup> Hideki Ishihara,<sup>†</sup> and Yohsuke Takamori<sup>‡</sup>*Department of Mathematics and Physics, Graduate School of Science, Osaka City University, Osaka 558-8585, Japan*

(Received 28 December 2010; published 2 February 2011)

We study bound orbits of a free particle around a singly rotating black ring. We find there exists chaotic motion of a particle which is gravitationally bound to the black ring by using the Poincaré map.

DOI: 10.1103/PhysRevD.83.047501

PACS numbers: 04.50.Gh

**I. INTRODUCTION**

Chaos is one of the characteristic behaviors of nonlinear dynamical systems. In the context of general relativity, there are two main issues concerning chaos. One is chaotic oscillations which generally occur in the early stage of the universe near the initial singularity [1,2]. The other is chaotic motion of particles around black holes. There appears chaotic behavior of charged particles around a magnetized black hole [3], particles around a gravitationally perturbed black hole [4], a spinning particle around a black hole in vacuum [5], and particles around multiple black holes [6].

Recently, general relativity in higher dimensions has gathered much attention in relation to modern unified theories of interactions. Properties of the gravitational field depend on the spacetime dimensions critically. As for the cosmological models, the chaotic oscillations of the early universe disappear in higher dimensions [7]. As for the black holes, in five dimensions, exact solutions of a black ring with the horizon topology of  $S^2 \times S^1$  are discovered by Emparan and Reall [8] in addition to rotating black holes with the spherical horizon topology obtained by Myers and Perry [9].

The geodesic motion of a test particle is one of the most important probes for spacetime geometry because it reveals the geometrical difference of the black ring and the black hole. It is known that Myers-Perry black holes in any dimensions allow separation of variables in the Hamilton-Jacobi equation for geodesics [10] as well as the Kerr black hole in four dimensions. This occurs because of the existence of a rank-2 Killing tensor in addition to Killing vectors generating isometries. However, the separation of variables in the black ring geometry does not occur by the ring coordinates [11,12]. As another interesting difference, the black rings have stable bound orbits of a particle [13], while the black holes in five dimensions do not. This comes from the difference of shapes of black objects.

If the particle motion bounded in a finite region is not integrable, the following natural question arises. Is the particle motion chaotic? The nonseparability of variables

in the black ring geometry suggests that there is no additional constant of motion except constants associated with the Killing vectors. However, we cannot conclude the absence of an additional constant of motion immediately because the Hamilton-Jacobi method depends on the choice of variables. In this report, we show the black ring geometry has chaotic bound orbits by using the Poincaré map. Appearance of the chaos implies the absence of an additional constant of motion in the black ring metric.

**II. GEOMETRY OF THE BLACK RING**

In terms of ring coordinates  $(t, x, y, \phi, \psi)$ , the black ring metric is given by

$$ds^2 = -\frac{F(y)}{F(x)} \left( dt - CR \frac{1+y}{F(y)} d\psi \right)^2 + \frac{R^2}{(x-y)^2} F(x) \times \left( -\frac{G(y)}{F(y)} d\psi^2 - \frac{dy^2}{G(y)} + \frac{dx^2}{G(x)} + \frac{G(x)}{F(x)} d\phi^2 \right), \quad (1)$$

where

$$F(\xi) = 1 + \lambda\xi, \quad G(\xi) = (1 - \xi^2)(1 + \nu\xi), \quad (2)$$

$$C = \sqrt{\lambda(\lambda - \nu) \frac{1 + \lambda}{1 - \lambda}}, \quad (3)$$

where the parameter  $R$  denotes the radius of the black ring, and  $\lambda$  and  $\nu$  characterize the rotation velocity and the thickness of the ring, respectively. The ranges of the parameters are

$$0 < R, \quad 0 < \nu \leq \lambda < 1, \quad (4)$$

and the ranges of the ring coordinates are given by

$$-\infty \leq y \leq -1, \quad -1 \leq x \leq 1. \quad (5)$$

In the black ring metric (1),  $y = -1/\nu$  is the position of the event horizon which has the topology of  $S^2 \times S^1$ . The metric admits three Killing vectors,  $\partial_t$ ,  $\partial_\psi$ , and  $\partial_\phi$ . The

<sup>\*</sup>igata@sci.osaka-cu.ac.jp

<sup>†</sup>ishihara@sci.osaka-cu.ac.jp

<sup>‡</sup>takamori@sci.osaka-cu.ac.jp

ring axis, fixed points of the rotation generated by  $\partial_\psi$ , is  $y = -1$ , and the equatorial plane, fixed points of the rotation generated by  $\partial_\phi$ , is  $x = \pm 1$ . The ergosurface exists at  $y = -1/\lambda$ , i.e., the Killing vector  $\partial_t$ , which is timelike at the spatial infinity, becomes null there. In terms of regularity condition at the ring axis and the equatorial plane,  $\lambda$  has to be chosen as

$$\lambda = \frac{2\nu}{1 + \nu^2}, \quad (6)$$

then the regular black ring solutions have two free parameters  $R$  and  $\nu$ .

### III. PARTICLE MOTION AROUND THE BLACK RING

The Hamiltonian of a free particle with mass  $m$  is generally given by

$$H = \frac{N}{2}(g^{\mu\nu} p_\mu p_\nu + m^2), \quad (7)$$

where  $N$  is the Lagrange multiplier and  $p_\mu$  is the canonical momentum. In the case of particle motion around the black ring metric (1), since  $t$ ,  $\psi$ , and  $\phi$  are cyclic coordinates, then the conjugate momenta  $p_t$ ,  $p_\psi$ , and  $p_\phi$  are constants of motion. Then, the geodesic Hamiltonian is reduced in the form

$$H = \frac{N}{2} \left[ g^{xx} p_x^2 + g^{yy} p_y^2 + E^2 \left( U_{\text{eff}} + \frac{m^2}{E^2} \right) \right], \quad (8)$$

where

$$U_{\text{eff}} = g^{tt} + g^{\phi\phi} l_\phi^2 + g^{\psi\psi} l_\psi^2 - 2g^{t\psi} l_\psi \quad (9)$$

with

$$\begin{aligned} g^{tt} &= -\frac{F(x)}{F(y)} - \frac{C^2(x-y)^2(y+1)^2}{G(y)F(x)F(y)}, \\ g^{xx} &= \frac{(x-y)^2}{R^2} \frac{G(x)}{F(x)}, \\ g^{yy} &= -\frac{(x-y)^2}{R^2} \frac{G(y)}{F(x)}, \\ g^{\phi\phi} &= \frac{(x-y)^2}{R^2 G(x)}, \\ g^{\psi\psi} &= -\frac{F(y)(x-y)^2}{R^2 G(y)F(x)}, \\ g^{t\psi} &= -\frac{C(x-y)^2(y+1)}{RG(y)F(x)}, \end{aligned} \quad (10)$$

and  $E = -p_t$ ,  $l_\phi = p_\phi/E$ , and  $l_\psi = p_\psi/E$  are constants.

By variation of the geodesic action with  $N$ , we obtain the Hamiltonian constraint condition

$$g^{xx} p_x^2 + g^{yy} p_y^2 + E^2 \left( U_{\text{eff}} + \frac{m^2}{E^2} \right) = 0. \quad (11)$$

In what follows, to give more intuitive pictures of particle motion, we use  $\zeta$ - $\rho$  coordinates which are defined as

$$\zeta = R \frac{\sqrt{y^2 - 1}}{x - y}, \quad \rho = R \frac{1 - x^2}{x - y}. \quad (12)$$

In these coordinates, the flat metric takes the form

$$ds^2 = -dt^2 + d\zeta^2 + \zeta^2 d\psi^2 + d\rho^2 + \rho^2 d\phi^2. \quad (13)$$

The ring axis and the equatorial plane correspond to  $\zeta = 0$  and  $\rho = 0$ , respectively, and the horizon of the black ring  $y = -1/\nu$  is represented by a circle on the equatorial plane. The effective potential  $U_{\text{eff}}$  is a function of  $\zeta$  and  $\rho$  with the parameters  $\nu$ ,  $l_\psi$ , and  $l_\phi$ .

As is shown in the previous work [13], if  $l_\phi$  and  $l_\psi$  are chosen in a suitable range, the effective potential  $U_{\text{eff}}$  has a local minimum at a point, say  $(\zeta_s, \rho_s)$ , i.e., there exist stable bound orbits around the black ring. The projection of each orbit on a time slice is a toroidal spiral curve on the two-dimensional torus, direct product of  $S^1$  with radius  $\zeta_s$  and  $S^1$  with radius  $\rho_s$ . In the case that  $l_\psi = 0$ , a potential minimum appears on the ring axis  $\zeta = 0$ . A minimum point on the ring axis ( $\zeta_s = 0, \rho_s$ ) implies a stable circular orbit of the radius  $\rho_s$  on the ring axis. There also exist potential minima off the ring axis for some  $l_\phi$ . It means that the orbits with  $l_\psi = 0$  can take toroidal spiral shapes because of dragging by the rotation of black rings.

### IV. CHAOTIC MOTION

Now, we observe the appearance of chaotic behavior of bound orbits around the black ring. We consider dynamical geodesic motion bounded in a finite region. Such orbits exist near the stable bound orbits. In Fig. 1, we show typical orbits in the  $\zeta$ - $\rho$  plane with contours of  $U_{\text{eff}}$  by solving the equations of motion numerically. We find a saddle point of  $U_{\text{eff}}$  between the local minimum and the horizon (see Fig. 1). The particle motion with the energy  $E$  in the range

$$E_s \leq E < E_u \quad (14)$$

is bounded in a finite region around the local minimum, where  $E_s$  and  $E_u$  are energy levels of the local minimum (stable point) at  $(\zeta_s, \rho_s)$  and the saddle point (unstable point) of  $U_{\text{eff}}$ , respectively. If the energy of the particle is a little bit larger than  $E_s$  such that the particle orbit is confined in a vicinity of the local minimum, the orbit makes a Lissajous figure. As the energy  $E$  increases, the Lissajous figure is deformed, and in the case that the energy becomes as large as  $E_u$  such that particle can approach the saddle point of  $U_{\text{eff}}$ , the orbits become complicated and irregular.

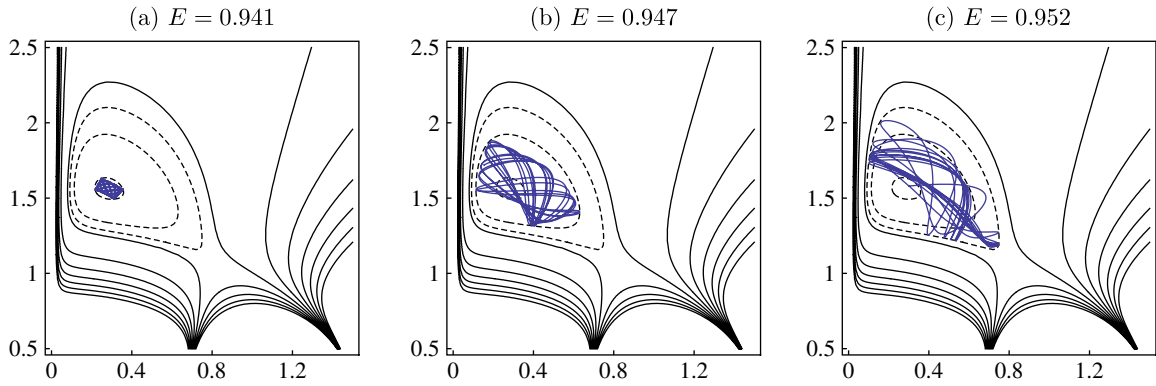


FIG. 1 (color online). Orbits of a particle are plotted on the  $\zeta$ - $\rho$  plane with contours of the effective potential  $U_{\text{eff}}$ . The horizontal axis denotes  $\zeta$  and the vertical axis denotes  $\rho$ . The parameters are set as  $\nu = 0.4$  and  $R = 1$  for the black ring geometry, and  $l_\phi = 1.52$  and  $l_\psi = 0.02$  for constants of motion. Energies are (a)  $E = 0.941$ , (b)  $E = 0.947$ , and (c)  $E = 0.952$ . The energy levels of the orbits are shown by broken closed curves.

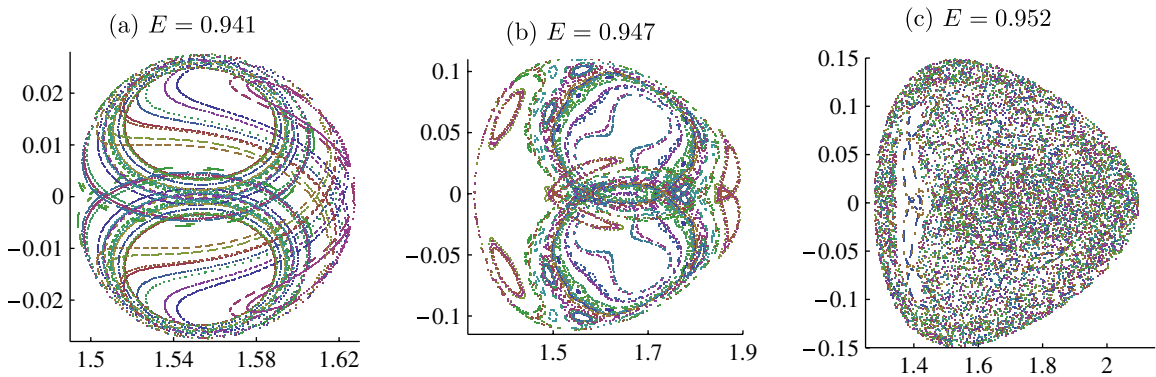


FIG. 2 (color online). The Poincaré maps with the surface of section  $\zeta = \zeta_s = 0.3$  are shown in the  $\rho$ - $p_\rho$  plane. The horizontal axis is  $\rho$  and the vertical axis is  $p_\rho$ . The parameters are the same as in Fig. 1. Thirty orbits with different initial conditions are superposed in each panel.

To inspect the trajectories in the phase space  $(\zeta, \rho, p_\zeta, p_\rho)$ , we use the Poincaré map. We plot intersections of a trajectory by the surface of section  $\zeta = \zeta_s$  with  $p_\zeta > 0$  on the two-dimensional  $\rho$ - $p_\rho$  plane (see Fig. 2). In the low energy case, we see the plotted points lie on a closed curve in the  $\rho$ - $p_\rho$  plane. As the energy  $E$  increases, the closed curve in the Poincaré map is modulated and broken. In the high energy case, sections of a single trajectory fill a finite region. The behavior of the Poincaré map which depends on the energy of the particle is the

same as the Hénon-Heiles system [14]. The scattered points of the Poincaré map imply the particle motion is chaotic. Therefore, we can conclude that there is no additional constant of motion except the energy and the angular momenta which are related to the isometries of the metric.

## ACKNOWLEDGMENTS

This work is supported by the Grant-in-Aid for Scientific Research No. 19540305.

- 
- [1] V. A. Belinskii, I. M. Khalatnikov, and E. M. Lifshits, *Adv. Phys.* **19**, 525 (1970).  
 [2] A. B. Burd, N. Buric, and G. F. R. Ellis, *Gen. Relativ. Gravit.* **22**, 349 (1990); D. Hobill, D. Bernstein, M.

Welge, and D. Simkins, *Classical Quantum Gravity* **8**, 1155 (1991); E. Calzetta and C. El Hasi, *Classical Quantum Gravity* **10**, 1825 (1993); A. Burd and R. Tavakol, *Phys. Rev. D* **47**, 5336 (1993).

- [3] H. Varvoglis and D. Papadopoulos, *Astron. Astrophys.* **261**, 664 (1992); V. Karas and D. Vokrouhlicky, *Gen. Relativ. Gravit.* **24**, 729 (1992).
- [4] L. Bombell and E. Calzetta, *Classical Quantum Gravity* **9**, 2573 (1992); R. Moeckel, *Commun. Math. Phys.* **150**, 415 (1992); A. P. S. de Moura, *Phys. Rev. E* **61**, 6506 (2000).
- [5] S. Suzuki and K. Maeda, *Phys. Rev. D* **55**, 4848 (1997).
- [6] G. Contopoulos, *Proc. R. Soc. A* **431**, 183 (1990); **435**, 551 (1991); C. P. Dettmann, N. E. Frankel, and N. J. Cornish, *Phys. Rev. D* **50**, R618 (1994); *Fractals* **3**, 161 (1995); U. Yurtsever, *Phys. Rev. D* **52**, 3176 (1995); Y. Sota, S. Suzuki, and K. Maeda, *Classical Quantum Gravity* **13**, 1241 (1996).
- [7] H. Ishihara, *Prog. Theor. Phys.* **74**, 490 (1985); A. Tomimatsu and H. Ishihara, *Gen. Relativ. Gravit.* **18**, 161 (1986); A. Hosoya, L. G. Jensen, and J. A. Stein-Schabes, *Nucl. Phys.* **B283**, 657 (1987); Y. Elskens and M. Henneaux, *Classical Quantum Gravity* **4**, L161 (1987); J. Demaret, Y. De Rop, and M. Henneaux, *Phys. Lett. B* **211**, 37 (1988); *Int. J. Theor. Phys.* **28**, 1067 (1989).
- [8] R. Emparan and H. S. Reall, *Phys. Rev. Lett.* **88**, 101101 (2002).
- [9] R. C. Myers and M. J. Perry, *Ann. Phys. (N.Y.)* **172**, 304 (1986).
- [10] V. P. Frolov and D. Stojkovic, *Phys. Rev. D* **68**, 064011 (2003); V. P. Frolov, P. Krtous, and D. Kubiznak, *J. High Energy Phys.* **02** (2007) 005; V. P. Frolov and D. Kubiznak, *Phys. Rev. Lett.* **98**, 011101 (2007).
- [11] J. Hoskisson, *Phys. Rev. D* **78**, 064039 (2008).
- [12] M. Durkee, *Classical Quantum Gravity* **26**, 085016 (2009).
- [13] T. Igata, H. Ishihara, and Y. Takamori, *Phys. Rev. D* **82**, 101501(R) (2010).
- [14] M. Hénon and C. Heiles, *Astron. J.* **69**, 73 (1964).